Experiments Toward Non-contact Safety Standards for Automated Industrial Vehicles

Roger Bostelman, Tsai Hong, and Raj Madhavan

National Institute of Standards and Technology
Gaithersburg, MD 20899-8230
{roger.bostelman, tsai.hong, raj.madhavan}@nist.gov

Abstract: **The performance evaluation of an obstacle detection and segmentation algorithm is explained upon comparing a new range camera to ground truth. Automated Guided Vehicles (AGVs) in factory-like environments may one day utilize this algorithm for advanced vehicle navigation along with using a new 3D real-time range camera. Our approach expands on the US and British Safety Standards, which allow for non-contact safety sensors on vehicles, by performing tests on objects specifically sized in both standards. These successful tests placed the recommended, as well as smaller, material-covered and sized objects on the vehicle path for static measurement. The segmented (mapped) obstacles were then verified in range to the objects and object size using simultaneous, absolute, ground truth measurements obtained from a relatively accurate 2D scanning laser rangefinder. The 3D range cameras are expected to be relatively inexpensive, used indoors and possibly one day used outdoors for several potential mobile robot applications that build upon experimental results explained in this paper.**

Index Terms **— 3D range camera, real-time, safety standard, ground truth, obstacle segmentation, automated guided vehicle.**

I. INTRODUCTION

Obstacle detection and mapping are crucial for autonomous indoor driving. This is especially true for Automated Guided Vehicle (AGV) navigation in factory-like environments where safety of personnel and that of the AGV itself are of utmost importance. This paper describes the performance of an obstacle detection and segmentation algorithm using a 3D real-time range camera to detect safety standard-sized objects.

The 3D range camera[1] is based on the Time-Of-Flight (TOF) principle [8] and is capable of simultaneously producing intensity images and range information of targets in indoor environments. This range camera is extremely appealing for obstacle detection in industrial applications as, when it becomes commercially available, it is expected to be relatively inexpensive as compared to similar sensors and can deliver range and intensity images at a rate of up to 20 Hz with an active range of 7.5 m while incorporating no moving parts, such as a spinning mirror as in many off-the-shelf laser sensors.

Since obstacle detection plays a critical role in autonomous driving, there has been much research on many different types of sensors, such as sonar [14], color/gray level cameras [2], FLIR (Forward Looking InfraRed) cameras [14], and stereo cameras [13], [1], [16], [7]. Most of the vision approaches are not applicable to indoor scenes due to lack of texture in the environment. Other researchers have proposed LADAR (Laser Detection And Ranging) sensors for detecting obstacles [5], [4], [6]. However, one-dimensional LADAR, which has been used in the AGV industry, is not suitable for the 3D world of factory environments and other complex volumes without moving the sensor during operation.

Using AGVs a factory line can be active 24 hours a day with minimal human interaction. This kind of vehicle has been applied to tasks like movement of products in warehouses, distributions and storage functions or transport of subparts between different assembly stations in a production line [11]. Unless clear, designated facility areas are carved out for AGVs to operate within, as well as a fully structured vehicle routing plan implemented (fixed-path navigation), AGVs may not be safe and effective in flexible manufacturing facilities. In open path navigation, as opposed to fixed-path navigation, the AGV can, at least theoretically, take any path to navigate between points. This implies that the vehicle can sense its environment and plan paths through this 3D world. NIST is working in this area to hopefully open niche markets for robot vehicle vendors as well as, provide improved vehicle performance and capabilities to existing capital investments made by robot vehicle users. The 3D range camera discussed in this paper can provide, or augment existing sensor systems to provide, obstacle detection as needed for many industrial AGV needs.

---

[1] Commercial equipment and materials are identified in this paper in order to adequately specify certain procedures. Such identification does not imply recommendation or endorsement by the National Institute of Standards and Technology, nor does it imply that the materials or equipment identified are necessarily the best available for the purpose.

Our proposed approach to obstacle detection uses a low cost, 3D, real-time, range camera (CSEM SwissRanger 2). First, we calibrate the camera with respect to the AGV so that we can convert the range values to 3D point clouds in the AGV coordinate frame. Second, we segment the objects which have high intensity and whose elevation values are above the floor of the operating environment on the AGV path. The segmented 3D points of the obstacles are then projected and accumulated into a grid placed over the floor surface-plane. The algorithm utilizes the intensity and 3D structure of range data from the camera and does not rely on the texture of the environment. The segmented (mapped) obstacles are verified using absolute measurements obtained using a relatively accurate 2D scanning laser rangefinder (SICK LMS200). Our approach has been tested successfully on objects that approximate US and British safety standard recommended object sizes covered with cotton, cloth material and placed in the vehicle's path. The AGV remained stationary as the measurements were collected for this paper.

The U.S. American Society of Mechanical Engineers (ASME) B56.5-2004 standard [17] was recently changed to allow non-contact safety sensors as opposed to contact sensors such as bumpers to be used on AGVs. Prior to the change, the B56.5 standard defined an AGV bumper as a "mechanically actuated device, which when depressed, causes the vehicle to stop." With the current B56.5 standard change and with state-of-the-art non-contact safety sensors, vehicles can be shorter in length, excluding mechanical bumpers since these bumpers extend much farther in front and behind the vehicle than non-contact sensors. This in turn allows shorter vehicle turning radii and they can potentially move faster as objects can be detected well before the vehicle is close to an object. Ideally, the US and even the British [18] safety standards can be changed even further toward a unified, global safety standard for AGV's and other driverless vehicles.

The paper has five sections: Section II describes the concept of obstacle detection and segmentation including the 3D range camera, algorithm, and a modulation issue using range camera images. Section III provides the experimental setup and results when the proposed algorithm is employed for detection and segmentation of a British standard size and material-covered test apparatus. Section IV provides further discussion beyond the standards efforts towards typical indoor factory environment applications and indicates future research areas that are under investigation. Section V provides a summary and conclusion.

II. OBSTACLE DETECTION AND SEGMENTATION

A. 3D Range Camera

In this section, we describe an algorithm to detect and segment obstacles in the path of the AGV using a solid-state Time-Of-Flight (TOF) range camera. The 3D range camera shown in Figure 1 is a compact, robust and cost effective solid state device capable of producing 3D images in real time.

Figure 1 *- The TOF 3D range image camera. The camera simultaneously generates intensity images and range information of targets in its field-of view at a rate of 20 Hz with an active range of 7.5 m.*

The camera measures 14.5 x 4 x 3 cm (5.7 x 1.6 x 1.2 in), has a field-of-view of 46° (vertical) x 42° (horizontal), and is capable of producing range images of 160 x 124 pixels over a 7.5 m range. For a brief overview of the characteristics and operating principles of the camera, see [12].

The British EN1525 safety standard specifies that horizontal test pieces used to test sensors shall be 200 mm in diameter x 600 mm long lying perpendicular to the vehicle path. Vertical test pieces shall be 70 mm in diameter by 400 mm tall and completely within the vehicle path. Approximately sized British standard test obstacles, as shown in Figure 2 (a and b), were placed on the travel path for our experiments.

B. Algorithm Details

The obstacle detection algorithm processes the range data and determines not only the obstacle range, but also segments the obstacles from their environment and places them in a model of the world (maps). The algorithm combines intensity and range images from the range camera to detect the obstacles and estimate the distance to the obstacles.

We first calibrate the camera with respect to the AGV so that we can convert the range values to 3D points in the AGV coordinate frame. Next, we segment the objects which have high intensity and whose elevation values are above the floor of the operating environment on the AGV path. The segmented 3D points of the obstacles are then projected and accumulated into the floor surface-plane. The algorithm utilizes the intensity and 3D structure of range data from the camera and does not rely on the texture of the environment. The segmented (mapped) obstacles are verified using absolute measurements obtained using a 2D scanning laser rangefinder with a range uncertainty of 3 cm (1.2 in).

Specifically, the steps of the algorithm are illustrated for a sample image from the range camera:

1) a patch of data with high intensity values (i.e., greater than half of the average brightness of intensity value returned from the camera) in the front of the robot is used to fit a plane for estimating the floor surface as shown in Figure 3(a). In our experiments, the average intensity value returned from the camera is a robust threshold value to measure the goodness of range return. However, we believe that a learning algorithm should be implemented to learn the threshold value to optimize the best range returns on the floor or other environment areas.

2) the left and right edges of the 3D robot paths (the sensors and robot were stationary) are projected to the range and intensity images such that only obstacles on the path (i.e., the hallway) that can be considered as shown in Figure 3(b). The path is chosen and defined by the planner in our 4D/RCS (4-Dimensional, Real-time Control System) [18].

3) all the intensity pixels inside of the left and right edges are used to hypothesize the potential obstacle. If the intensity value of the pixel is greater than half of the average of the intensity in the image, then the pixel is considered as a potential obstacle as shown in Figure 3(c).

4) each potential obstacle pixel in the range image is used to find the distance to the floor plane when the distance to the floor is greater than a user-defined threshold as shown in Figure 3(d). The threshold is dependent on the traversability (ground clearance) of the robot and sensor placement with respect to the floor.

(a) (b)

Figure 2 *- Experimental setup (a) vertical test apparatus where the center object most closely matches the British standard size test piece measuring 65 mm dia. x 400 mm long. The remaining vertical objects are all thinner. (b) horizontal test apparatus (mannequin leg) measuring a segment approximately tapered from 80 to 160 mm dia. x 600 mm long including the leg ankle to the thigh. In both (a) and (b), objects are covered in cloth as also specified in the standard. See Section III Experimental Setup and Results for further details.*

Potential obstacles in the world model can be accumulated as the AGV drives. Figure 4 (right) shows an obstacle map representation that is part of the world model. The obstacles map is shown at 10 cm grid resolution. Nearly all the obstacles are found, although at the cost of false positives from the reflected objects. To increase the accuracy of obstacle detection, the obstacles in the map and information obtained from an added color camera may be temporally integrated. Such integration has proven to be a very useful cue for obstacle detection [9].

C. Modulation Issue

An issue with this particular range camera is the modulation of returned data at approximately 7.5 m. Within the range of approximately 7.5 m, the camera accurately senses (to within 3 mm) the range to objects. Beyond 7.5 m, the camera continues to sense objects although it places the object data within the modulation of 7.5 m. For example, an object detected at 11 m would be placed in the returned data at a range of (11 m – 7.5 m =) 3.5 m (see Figure 5).

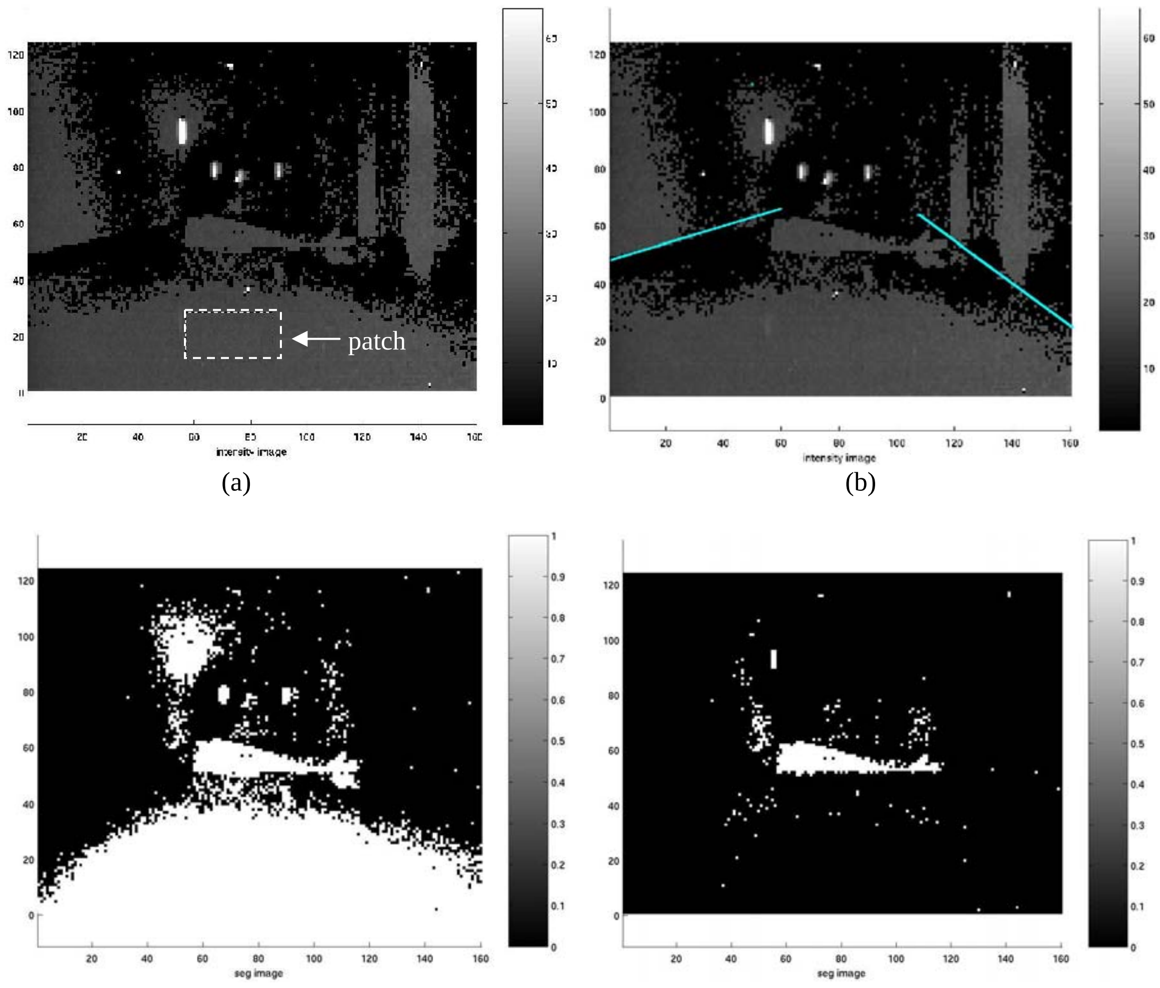

Figure 3 *- Obstacle segmentation algorithm illustration.*

To eliminate the modulation issue, a lower emitted light modulation frequency (ELMF) below the typical 20 MHz can be used to establish a longer, yet lower accuracy (as stated by the manufacturer) range modulation and could be used to compare with the 7.5 m range modulated range data. The compared data within the two modulation frequencies can then be used to mask objects detected beyond the 7.5 m range. Also, similar to how humans have and use peripheral vision, these longer-range objects created by a higher ELMF setting could be placed in the world model for additional (though higher uncertainty) environmental information. A human's peripheral vision provides excellent motion detection [8], the higher ELMF setting could produce low relative accuracy, yet larger range and volume (see Figure 5) motion detection of obstacles beyond the 7.5 m specified by the manufacturer. While the disadvantage here is producing higher relative range uncertainty, the advantage for vehicle control is that decisions can be made much earlier to react to potential obstacles farther away, even if their exact range is unknown.

III. EXPERIMENTAL SETUP AND RESULTS

The experiments were conducted under two scenarios as stated within the European British Standard:

- A test apparatus with a diameter of 200 mm and a length of 600 mm placed at right angles on the path of the AGV.
- A test apparatus with a diameter of 70 mm and a height of 400 mm set vertically within the path of the AGV.

Figures 2(a) and (b) show the experimental setup for the two aforementioned scenarios. The camera lens was centered approximately horizontally and vertically on the apparatus for all measurements. The scanning laser rangefinder was offset 250 mm below the camera. The range camera was used to detect the known test apparatus mounted on a stand and moved to different locations with respect to the camera.

The obstacle detection and segmentation algorithm was tested on two US/British standard test apparatuses as described in [17, 18], and was evaluated against ground truth to the apparatuses, which were placed at various distances between 0.5 m and 7.5 m from the sensor. A single-line, scanning laser rangefinder, shown in Figure 6, mounted below the range camera, simultaneously verified the distance to the test apparatus for each data set and served as ground truth. The rangefinder produced 401 data points over a 100° semi-circular region in front of the robot with each scan.

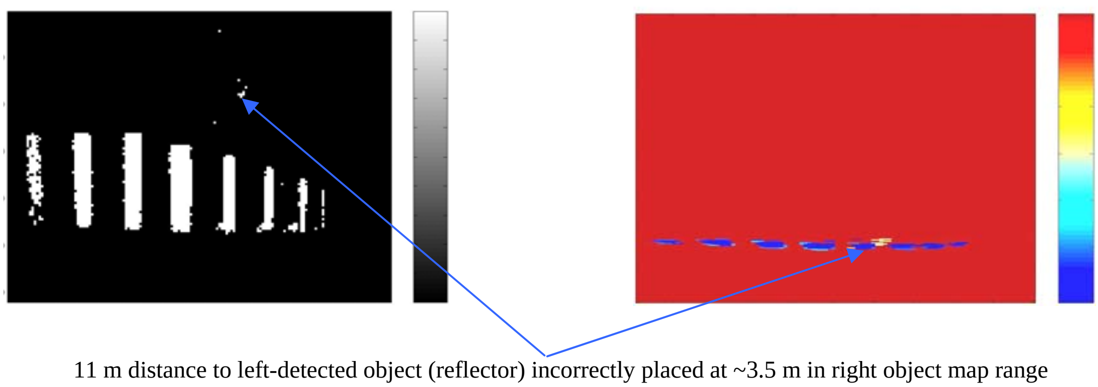

(a) (b)

***Figure 4** – (a) Segmented obstacles and (b) obstacle map but, due to range modulation, obstacles detected beyond 7.5 m max. camera range are placed within the 7.5 m range.*

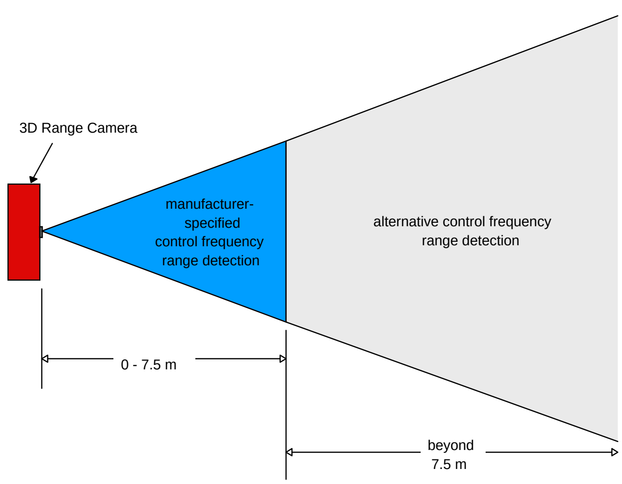

***Figure 5** – Graphic depicting range information (left) versus potential range information (right) with an alternative emitted light modulation frequency.*

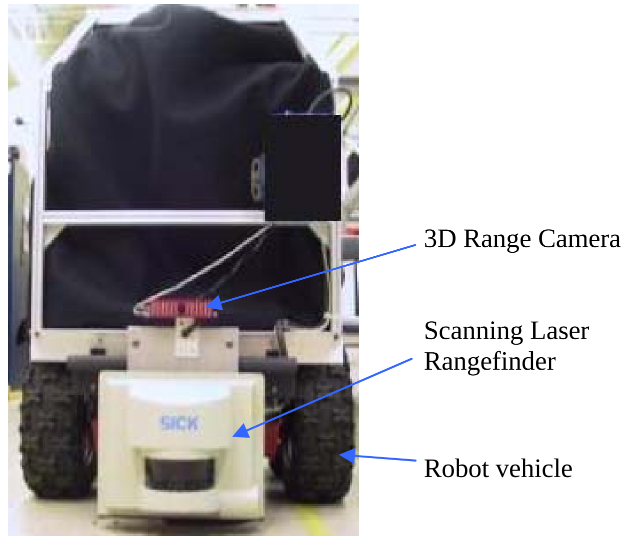

Figure 6 *- Experimental setup of the AGV, the scanning laser rangefinder, and the range camera.*

Table 1 shows the performance of the range camera for detecting the distance to the test apparatus placed at several distances from the range camera up to approximately 3 m. Between 3 m and 7.5 m, testing is continuing as camera settings were not optimized for these ranges. As shown in the table, the accuracy (mean) of the range decreases as the distance of the apparatus placed in front of the range camera is increased.

Table 1 *- Quantitative Comparison of Performance*

Nominal Obstacle Distance (cm)	*3D Range Camera Mean (cm)*	*2D Rangefinder Mean (cm)*
64	64.076	64.662
111	111.039	111.316
160	161.390	160.690
210	204.004	210.000
259	249.499	259.143
310	284.703	310.158

Figure 7 shows the test apparatus placed at a distance of 2.5 m from the range camera. Each object in the test apparatus was clearly detected even though the range camera also detected the reflectors on the hallway wall. Figures 7 (a, b, and c) show the resultant intensity, range, and segmented images, respectively. Figure 7(d) shows the ground truth provided by the scanning laser rangefinder rotated to show a top-down view.

Similar to Figure 3, we have previously shown in [10] additional data taken with a mannequin leg placed on the floor and with an approximate diameter of 200 mm and a length of 600 mm at the leg thigh region. This test apparatus is more challenging for the algorithm because the entire object is close to the floor. The legs are detected, but at the cost of detecting farther objects. Again, this deficiency can be eliminated by using two different modulation frequencies (such as 10 MHz and 20 MHz) where the detected objects would be coarsely represented at a more appropriate distance. The control algorithm can then intelligently delete them.

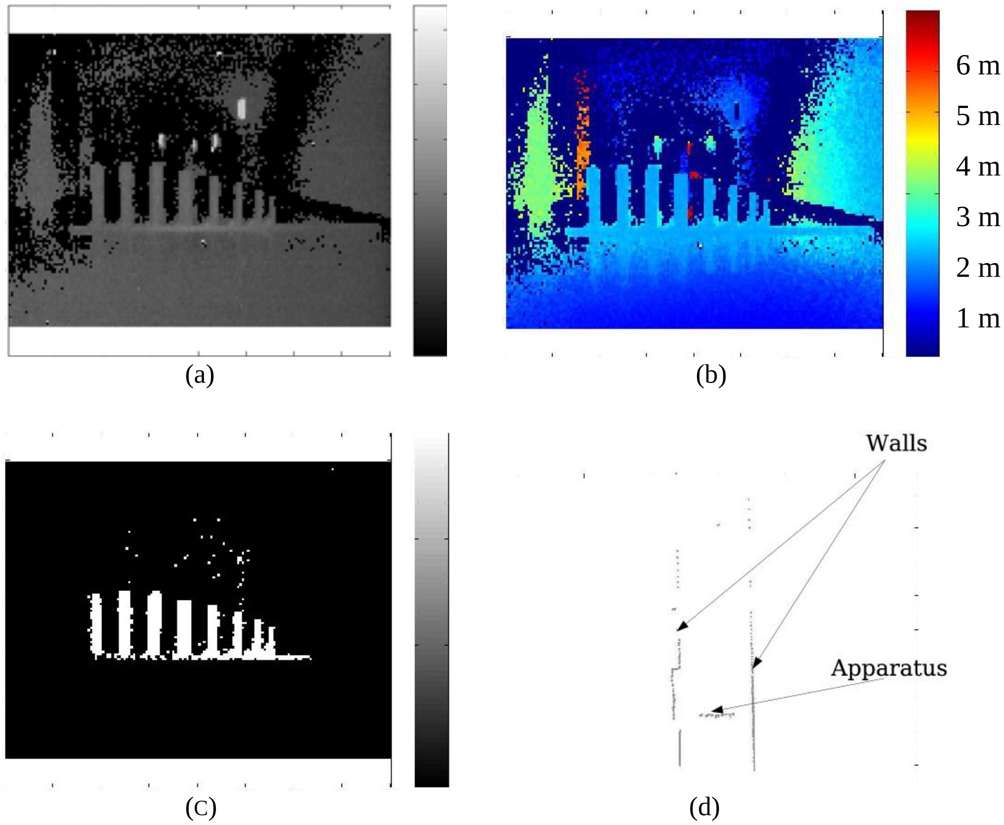

Figure 7 *- Results of the obstacle detection and segmentation algorithm for the experimental setup shown in Figure 2(a). The resultant intensity, range, and segmented images are shown in (a), (b) and (c), respectively. The ground truth provided by the scanning laser rangefinder is shown in (d) and has been rotated to show a top-down view.*

IV. FURTHER RESEARCH

A. Sensor Mount

Critical to the sensor itself is the mounting configuration of the sensor to enable detection of objects within the vehicle path and without sensor motion during critical detect times (e.g., scanning left exactly when a person enters the vehicle path from the right). Although there are no specific guidelines within the US safety standard for sensor mounts, it does suggest that the sensor be "fail-safe," and specifically regarding bumpers, that they "shall activate from a force applied parallel to the floor." The authors address this point further in [3] with potential mounting configuration of sensors surrounding the vehicle and experimental data showing results from two combined 3D range cameras into a single wide field of view (FOV) data set.

B. Industrial 3D Range Camera Applications Tests and Results

In an effort to move vehicles into industry beyond typical indoor AGV applications and toward increased robot navigational intelligence, the 3D range camera was used in a variety of settings: hallways (as previously shown and discussed in sections 1-3), room to room, loading docks and even outdoors.

Moving vehicles from indoors to outdoors could open a wide area of applications, including material handling to and from indoors and outdoors to a staging area or into another building, where safety sensors may become necessary and require alternative sensing capability. Outdoor tests were discussed in [3] as a starting point to our outdoor 3D range camera research. Although the 3D range camera manufacturer has stated that the camera is currently only reliable when used during indoor lighting conditions, the authors felt that a minimal inclusion in [3] was relevant to current AGV applications where sunlight may even enter the indoor facility.

To study room to room movement of AGVs and other mobile robots, we again used the 3D range camera mounted on the NIST Industrial Autonomous Vehicle (IAV) Testbed, a testbed used to study industrial mobility applications, shown in Figure 8(a) to capture the scene in Figure 8(b). The scene shows the robot pointing the 3D range camera at one of two open doors and through the door into a hallway where the apparatus for testing the US and British safety standards was placed. As shown in the intensity and range data in Figure 8(c and d), the robot can clearly detect the opening, closed door, test apparatus and even details of the apparatus including the small to large posts and mannequin arm. The approximate distances of these scene features (closed door = 3 m, apparatus = 4m, far wall = 5 m), measured roughly with a tape measure, closely mimic their measured ranges sensed by the 3D range camera.

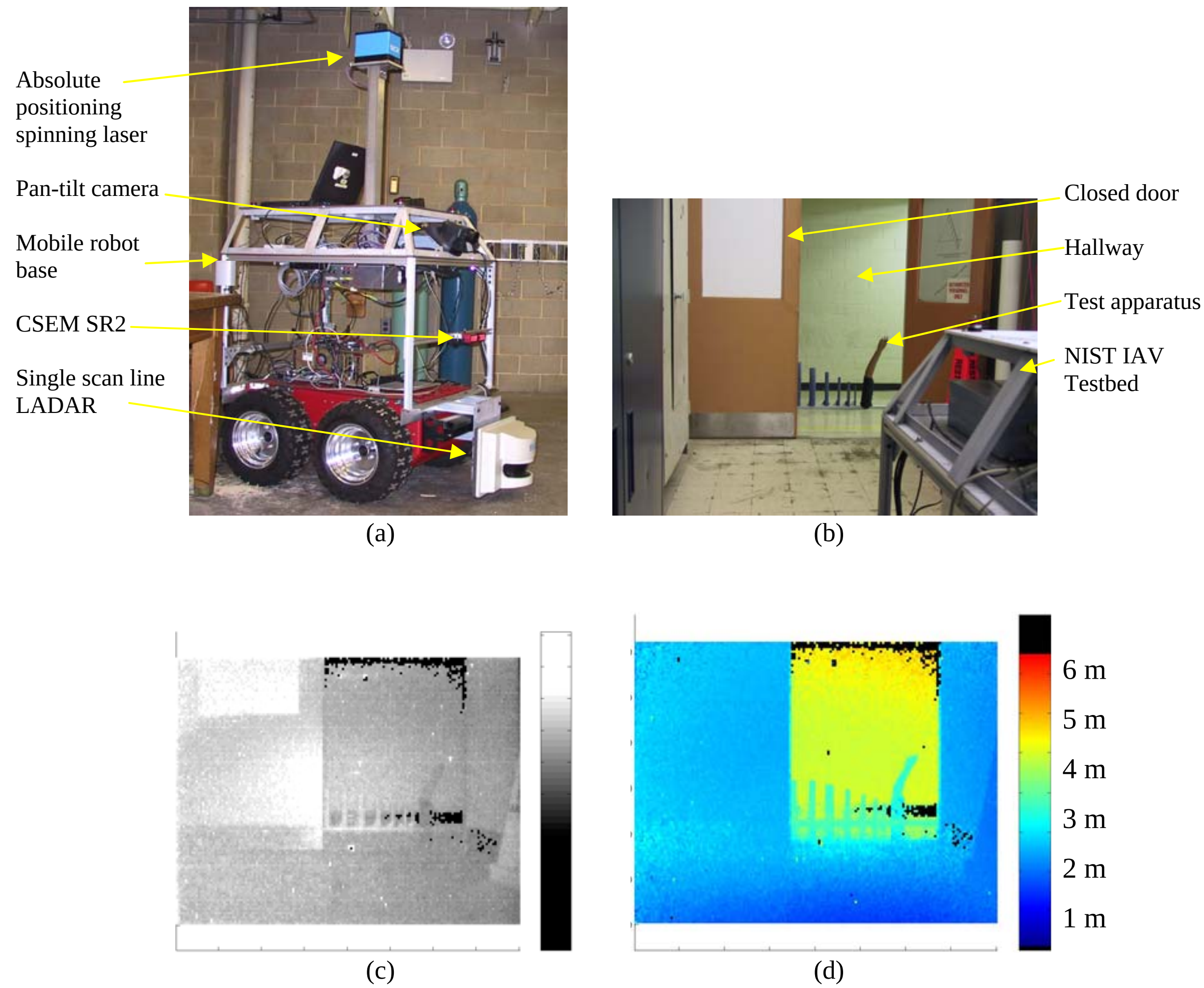

Figure 8 *– (a) NIST Industrial Autonomous Vehicle Testbed on which the 3D range camera and other sensors are mounted, (b) room to room test scene showing an open and closed door leading to a hallway and the standard test apparatus place in the hall, (c) 3D range camera intensity data of the scene, (d) 3D range camera range data.*

Industrial warehouses and other facilities typically have a loading dock similar to what is shown in Figure 9(a). The loading dock can have boxes and pallets as shown. In an unstructured environment such as this, pallets are placed randomly in the facility and manually moved from the loading dock to their destinations within or outside the facility by hand or using fork trucks and other material handling equipment. Ideally, these randomly placed pallets and boxes would be moved in and out of the loading dock area using AGVs without the need to precisely position the pallets or boxes for AGV access. The 3D range camera was used to detect the scene shown in Figure 9(a) to receive range data and to identify the boxes and the pallets. Much of the room was also within the 3D range camera's FOV and would need to be isolated from the pallets and boxes should an AGV be used for this operation.

On the left of Figure 9(a) are two boxes with no pallets beneath them. To the right of the two boxes are two pallets with boxes on them. The 3D range camera was used to verify a priori knowledge of pallet sizes, shapes and forklift pickup holes, and the results are shown in Figure 9(b and c) as intensity and range images. In addition, behind the boxes and pallets are shelves where empty pallets are stored, and above the boxes and pallets are low-hanging ducts. In the range data in Figure 9(c), these other objects are clearly identified as being farther away from the sensor than the pallets and boxes,. Therefore, with one image from the 3D range camera, the front boxes and pallets can be determined accessible by tall material handling equipment and the back shelves may be determined inaccessible with the same equipment. A single-line, scanning LADAR without a tilting mechanism would probably not be able to provide the same information. Although it may be able to detect the front pallets and boxes, it would not be able to distinguish between two objects with the same width but different heights. Several examples of LADARs that would provide appropriate 3D range imagery are discussed in [19].

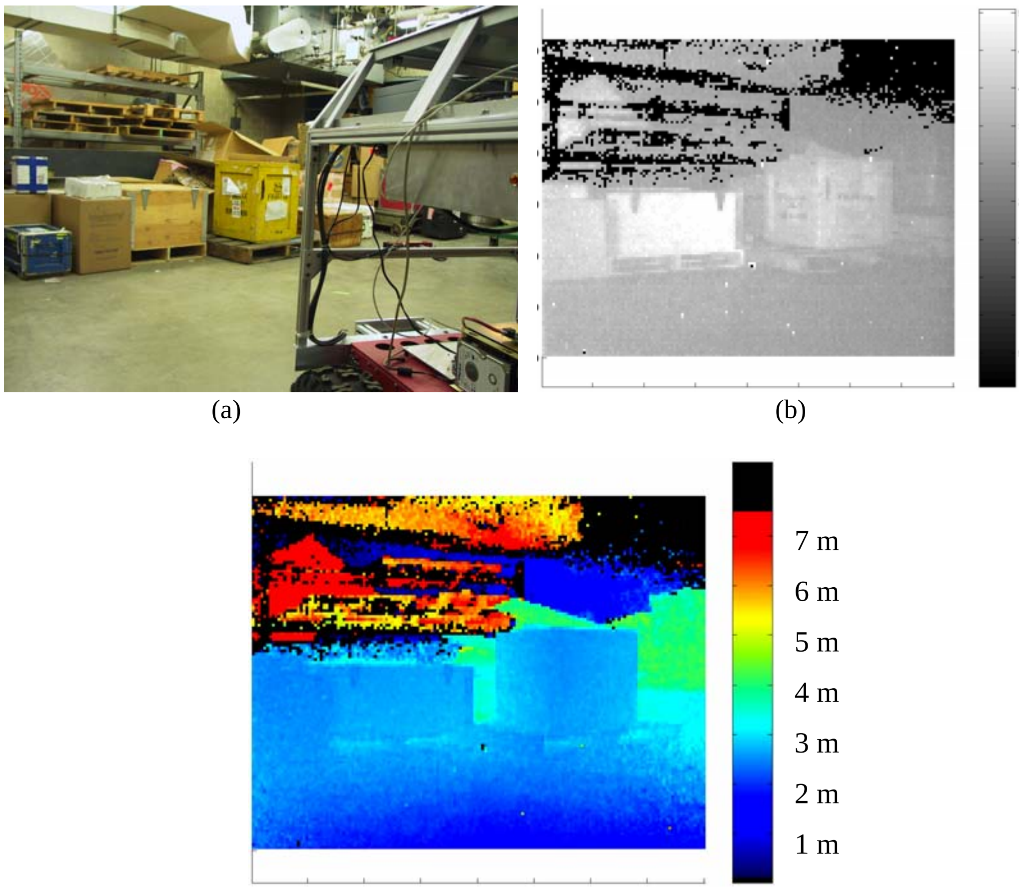

Figure 9 *- (a) Loading Dock scene used to test the 3D range camera to distinguish between boxes and pallets at a distance of approximately 3 m, (b) intensity data of the scene, (c) segmented range data. Note pallet holes, rear shelves and pallets, overhead objects, and other objects are also detected.*

In loading docks similar to that shown in Figure 9(a), forklifts and workers typically gain access to the dock through a garage door (see Figure 10(a)). A single-line, scanning LADAR without a tilting mechanism would not be able to detect a partially open door. The scenario is therefore better suited for a 3D sensor. The authors captured the range data shown in Figure 10(b) for this scene to verify whether or not the 3D range camera could detect the partially open door. Bright light on the floor caused by daylight entering through the open door can be seen in Figure 10(a). Although the 3D range camera used in these experiments is not suited for outdoor conditions, it was able to detect objects above the lighted area within its FOV, and the range image clearly shows that the door is not fully open. Just as the floor was stripped away using the object segmentation algorithm described earlier, the bright light on the floor in Figure 10(a) can also be removed. However, if the door were opened fully, allowing much more daylight to enter, the 3D range camera may have been blinded due to pixel saturation at the mounting height used. Should the 3D range camera be mounted higher, there may be no chance that sunlight may fully enter the 3D range camera, enabling it to always provide definitive knowledge of open or closed doorways. Therefore, mounting position of sensors on the robot is again critical and remains a function of the infinite number of facility access situations possible.

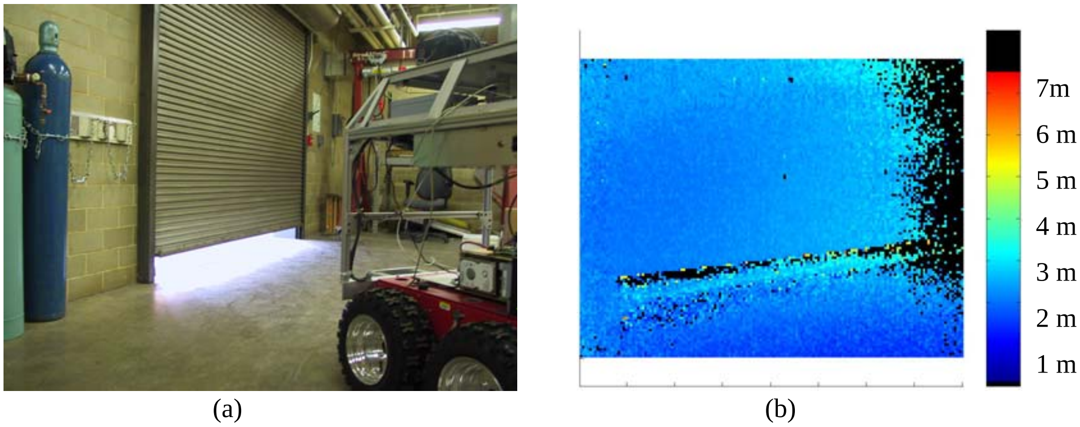

Figure 10 *- (a) Loading Dock garage door scene used to test the 3D range camera to determine whether the door is fully open or not to allow robot access, (b) range data of the scene showing noisy data where the open door was detected and clean data of the door above.*

V. SUMMARY AND CONCLUSIONS

An obstacle detection and segmentation algorithm for Automated Guided Vehicle (AGV) navigation in factory-like settings using a novel 3D range camera was described in this paper. The 3D range camera was used to detect standard sized objects referenced in US and British safety standards. The range camera is highly attractive for obstacle detection in industrial applications as it will be relatively cheap and can deliver range and intensity images in real-time for intelligent vehicle control. The performance of the algorithm was evaluated by comparing it with ground truth provided by a single-line, scanning laser rangefinder. A sensor modulation issue was described with a suggested remedy to allow objects beyond the 7.5 m modulation distance to be known or eliminated from the data.

Further research into issues beyond US and British standards efforts was also discussed, specifically: room to room, loading dock and open or closed door detection experiments using the 3D range camera. These particular locations and settings were chosen and tested as they represent difficult situations for single-line, scanning laser rangefinders on the market today. The 3D camera also requires carefully considering its mounting location and the lighting conditions of the environment in which it will operate so as not to saturate the detection circuitry (such as outdoor or indoor, bright conditions).

We envisage that the work discussed in this paper could be applied to:

- heavy manufacturing and industrial applications,
- moving obstacle detection for a moving AGV in indoor environments,
- detecting and tracking obstacles over long distances by combining the sensor with a color camera, and
- outdoor environments (provided that the sensor is redesigned to allow it to operate under bright light conditions).

Other prospective applications include: mapping factory environments after hours, manufacturing inside and outside during night (dark) hours, and space applications (due to the sensor's small weight and size).

VI. REFERENCES

[1] P. Batavia and S. Singh. Obstacle Detection Using Adaptive Color Segmentation and Color Stereo Homography. In Proc. of the IEEE Intl. Conf. on Robotics and Automation, May 2001.

[2] M. Bertozzi, A. Broggi, A. Fascioli, and P. Lombardi. Artificial Vision in Road Vehicles. In Proc. of the 28th IEEE Industrial Electronics Society Annual Conf., 2002.

[3] R. Bostelman, T. Hong, and R. Madhavan, Obstacle Detection using a Time-of-Flight Range Camera for Automated Guided Vehicle Safety and Navigation, to be published in the Integrated Computer-Aided Engineering Journal, 2005.

[4] T. Chang, T-H. Hong, S. Legowik, and M. Abrams. Concealment and Obstacle Detection for Autonomouos Driving. In Proc. of the Intl. Association of Science and Technology for Development - Robotics and Application, 1999.

[5] A. Ewald and V. Willhoeft. Laser Scanners for Obstacle Detection in Automotive Application. In Proc. of the Intell. Vehicles Symp., 2000.

[6] J. Hancock, M. Hebert, and C. Thorpe. Laser Intensity-based Obstacle Detection. In Proc. of the IEEE/RSJ Intl. Conf. on Intelligent Robots and Systems, 1998.

[7] M. Hariti, Y. Ruichek, and A. Koukam. A Voting Stereo Matching Method for Real-Time Obstacle Detection. In Proc. of the IEEE Intl. Conf. on Robotics and Automation, 2003.

[8] Hecht, Eugene, Optics, Schaum's Outline Series, McGraw-Hill ,1975

[9] T-H. Hong, T. Chang, C. Rasmussen, and M. Shneier. Feature Detection and Tracking for Mobile Robots Using a Combination of Ladar and Color Images. In Proc. of the IEEE Intl. Conf. on Robotics and Automation, May 2002.

[10] T. Hong, R. Bostelman, and R. Madhavan, Obstacle Detection using a TOF Range Camera for Indoor AGV Navigation, PerMIS 2004, Gaithersburg, MD, June 2004.

[11] H. Marbera, J. Quinonero, M. Izquierdo, A. ASkarmeta, “i-Fork: a Flexible AGV System using Topological and Grid Maps,” International Conference on Robotics and Automation, Taiwan, 2003.

[12] T. Oggier, M. Lehmann, R. Kaufmann, M. Schweizer, M. Richter, P. Metzler, G. Lang, F. Lustenberger, and N. Blanc. An All-solidstate Optical Range Camera for 3D Real-time Imaging with Subcentimeter Depth Resolution. In Proc. of the SPIE Conf. on Optical System Design, September 2003.

[13] C. Olson, L. Matthies, H. Schoppers, and M. Maimone. Robust Stereo Ego-motion for Long Distance Navigation. In Proc. of the IEEE Intl. Conf. on Computer Vision and Pattern Recognition, 2000.

[14] K. Owens and L. Matthies. Passive Night Vision Sensor Comparison for Unmanned Ground Vehicle Stereo Vision Navigation . In Proc. of the IEEE Intl. Conf. on Robotics and Automation.

[15] N. Sgouros, G. Papakonstantinous, and P. Tsanakas. Localized Qualitative Navigation for Indoor Environments. In Proc. of the IEEE Intl. Conf. on Robotics and Automation, 1996.

[16] R. Williamson and C. Thorpe. A Trinocular Stereo System for Highway Obstacle Detection. In Proc. of the IEEE Intl. Conf. on Robotics and Automation, 1999.

[17] American Society of Mechanical Engineers’ Safety Standard for Guided Industrial Vehicle and Automated Functions of Manned Industrial Vehicle. Technical Report ASME B56.5, 1993.

[18] British Standard Safety of Industrial Trucks - Driverless Trucks and their Systems. Technical Report BS EN 1525, 1998.

[19] W. Stone, M, Juberts, N. Dagalakis, J. Stone, J. Gorman. Performance Analysis of Next-Generation LADAR for Manufacturing, Construction, and Mobility, NISTIR 7117, May 2004.